DETERMINATION OF ROTORDYNAMIC COEFFICIENTS FOR LABYRINTH SEALS AND APPLICATION TO ROTORDYNAMIC DESIGN CALCULATIONS

P. Weiser and R. Nordmann
Department of Mechanical Engineering
University of Kaiserslautern
Kaiserslautern, Federal Republic of Germany

In today's rotordynamic calculations, the input parameters for a Finite Element Analysis (FEA) determine very much the reliability of Eigenvalue and Eigenmode predictions. While modelling of an elastic structure by means of beam elements etc. is relatively straightforward to perform and the input data for journal bearings are usually known exactly enough, the determination of stiffness and damping for labyrinth seals is still the subject of many investigations. Therefore, the rotordynamic influence of labyrinths is often not included in FEA for rotating machinery because of a lack of computer programs to calculate these parameters. This circumstance can give rise to severe vibration problems especially for high performance turbines or compressors, resulting in remarkable economic losses.
The forces generated in labyrinths can be described for small motions around the seal center with the linearized force-motion relationship of eq. 1:

$$\begin{bmatrix} K & k \\ -k & K \end{bmatrix} \begin{bmatrix} u_1 \\ u_2 \end{bmatrix} + \begin{bmatrix} D & d \\ -d & D \end{bmatrix} \begin{bmatrix} \dot{u}_1 \\ \dot{u}_2 \end{bmatrix} = - \begin{bmatrix} F_1 \\ F_2 \end{bmatrix} \tag{1}$$

where K, k are the direct and cross-coupled stiffness and D, d are the direct and cross-coupled damping. These elements are the so-called dynamic labyrinth coefficients.
Several years ago, we started with the development of computer codes for the determination of rotordynamic seal coefficients. The following sections will introduce our different approaches to evaluate the dynamic fluid forces generated by turbulent, compressible labyrinth seal flow.

NOMENCLATURE

K, k	Direct and cross-coupled stiffness	G	Labyrinth leakage
D, d	Direct and cross-coupled damping	r_a	Radius from seal center to stator
u_1, u_2	Rotor displacements		
$\dot{u}_1$, $\dot{u}_2$	Rotor velocities	r_i	Radius from seal center to end of seal fin
F_1, F_2	Labyrinth fluid forces		
Φ	General variable	x,y	cart. coordinates
Γ_Φ	Diffusion coefficient	$\bar{x},\bar{y}$	rot. coordinate system
S_Φ	Source term	w_i	preswirl
r, φ, z	Cylinder coordinates	τ	shear stress
η	Transformation coordinate	u,v,w	axial, radial and circumferential velocities
e	Perturbation parameter		
r_O	Rotor eccentricity		
Ω	Rotor precession frequency		
ω	Shaft rotational frequency		
h	Local seal clearance		
C_r	Nominal clearance		

Indices

0	Zeroth order	a	before labyrinth
1	First order	b	behind labyrinth

COMPUTATIONAL FLUID DYNAMICS METHODS (CFD)

The compressible, turbulent, time dependent and threedimensional flow in a labyrinth seal can be described by the Navier-Stokes equations in conjunction with a turbulence model. Additionally, equations for mass and energy conservation and an equation of state are required. These equations can be solved with the aid of a finite difference procedure. To determine the desired coefficients, two methods have been developed:

- 2-dimensional procedure based on a perturbation analysis
- 3-dimensional theory using a moving frame of reference rotating with the shaft.

PERTURBATION ANALYSIS

To describe the labyrinth seal flow, we use the time-averaged conservation equations for momentum, mass and energy and the equation of state for a perfect gas. The correlation terms of the turbulent fluctuation quantities are modeled via the k-ε turbulence model of LAUNDER and SPALDING /1/. All these equations can be arranged in the following generalized form:

$$\frac{\partial}{\partial t}(\rho\Phi) + \frac{\partial}{\partial z}(\rho u\Phi) + \frac{1}{r}\frac{\partial}{\partial r}(r\rho v\Phi) + \frac{1}{r}\frac{\partial}{\partial \varphi}(\rho w\Phi)$$
$$- \frac{\partial}{\partial z}\left(\Gamma_\Phi \frac{\partial \Phi}{\partial z}\right) - \frac{1}{r}\frac{\partial}{\partial r}\left(r\Gamma_\Phi \frac{\partial \Phi}{\partial r}\right) - \frac{1}{r}\frac{\partial}{\partial \varphi}\left(\frac{1}{r}\Gamma_\Phi \frac{\partial \Phi}{\partial \varphi}\right) = S_\Phi \qquad (2)$$

where Φ stands for any of the dependent variables(e.g. velocities, pressure, temperature, density), Γ_Φ is the diffusion coefficient and S_Φ the source term. To calculate the dynamic coefficients, several assumptions are introduced:

1. small rotor motions around the seal center on a circular orbit
2. coordinate transformation
3. perturbation series expansion for the dependent variables
4. solutions for the dependent variables corresponding to the temporal and circumferential variation of the seal clearance function

Assumption 1 assures that we can use eq. 1 to calculate the dynamic coefficients.
When supposing that the shaft rotates on a circular orbit, one can imagine that the local seal clearance h varies in time for every location φ=const. To avoid the use of time dependent calculation grids, we transform the governing equations to another coordinate system by introducing a new radial coordinate η whereby the eccentrically moving shaft is converted to a shaft rotating in the center of the seal (see Fig. 1).
The third assumption, together with assumption 1, implies that the perturbation series

$$\Phi = e^0\Phi_0 + e^1\Phi_1 + e^2\Phi_2 + \ldots + e^n\Phi_n \qquad n = 1 \ldots \infty \qquad (3)$$

for the dependent variables can be truncated after the linear term.

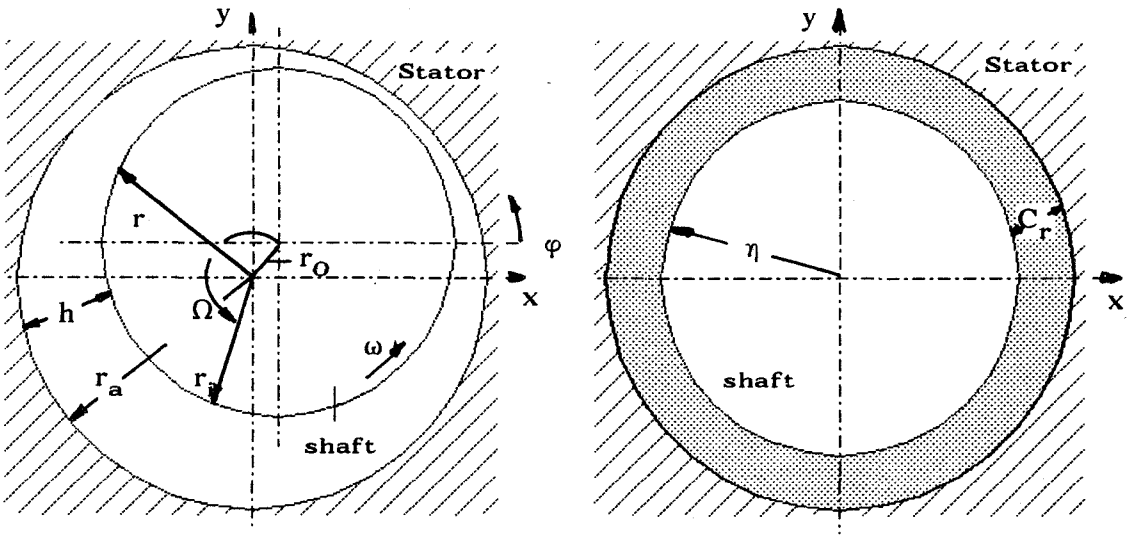

Fig. 1: Coordinate transformation

Inserting these equations for every dependent variable into the basic conservation relations yields two sets of equations. The zeroth order set describes the flow in the centric labyrinth while the first order equations are governing the flow field for small eccentric shaft motions. The last assumption allows the elimination of the temporal and circumferential derivatives in the first order equations analytically.

The seal clearance function for a circular shaft precession orbit around the seal center can be stated as

$$h = h_O + e\,h_1 = C_r - X(t)\cos\varphi - Y(t)\sin\varphi \qquad (4)$$

Corresponding to this function, we assume that the dependent variables vary in the same way concerning the circumferential direction.

Thereby, the circumferential derivatives can be calculated analytically. After separating the equations into sine and cosine terms and rearranging them by introducing complex variables, solutions for the first order variables corresponding to the temporal change of seal clearance due to a circular shaft orbit are prescribed, allowing the elimination of the derivatives with respect to time. Finally, we obtain two sets of differential equations which have to be solved subquently in order to determine the desired coefficients.

THREEDIMENSIONAL METHOD

In contrast to the perturbation analysis, where we have made many assumptions to reduce the computational effort, the threedimensional procedure shows much greater generality in avoiding these restrictions. Again, the time-averaged conservation equations are solved

in conjunction with the already mentioned k-ε model.
To determine the dynamic coefficients we assume that the shaft moves on a circular orbit with precession frequency Ω around the seal center. Since this would normally result in a time dependent problem we introduce a rotating coordinate system which is fixed at the shaft center (Fig. 2). In this moving frame of reference, the flow is stationary. Due to the rotating coordinate system, centrifugal and coriolis forces occur in the equations for radial and circumferential momentum.

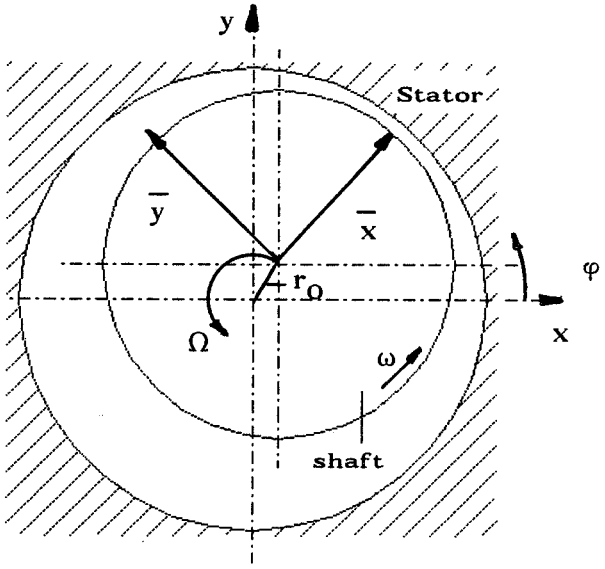

Fig. 2: Rotating coordinate system

SOLUTION PROCEDURE FOR THE CFD-METHODS

Because of the complexity of the derived equations, no analytic solution can be obtained. Therefore, there is a need for a numerical algorithm to solve the equations with the aid of a computer. We made our decision for the Finite Difference Method (FDM), which is well established in fluid dynamics.
The FDM procedure starts with the discretization of the calculation domain, which must be performed in a different manner for the two methods: While we can use a twodimensional Finite Difference grid for the perturbation analysis (Fig. 3), the threedimensional approach requires additional grids in the circumferential direction (Fig. 4).

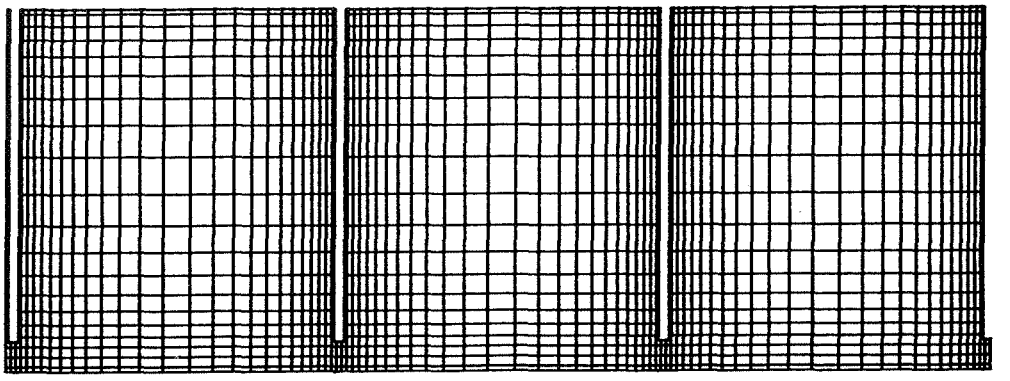

Fig. 3: Grid for perturbation method

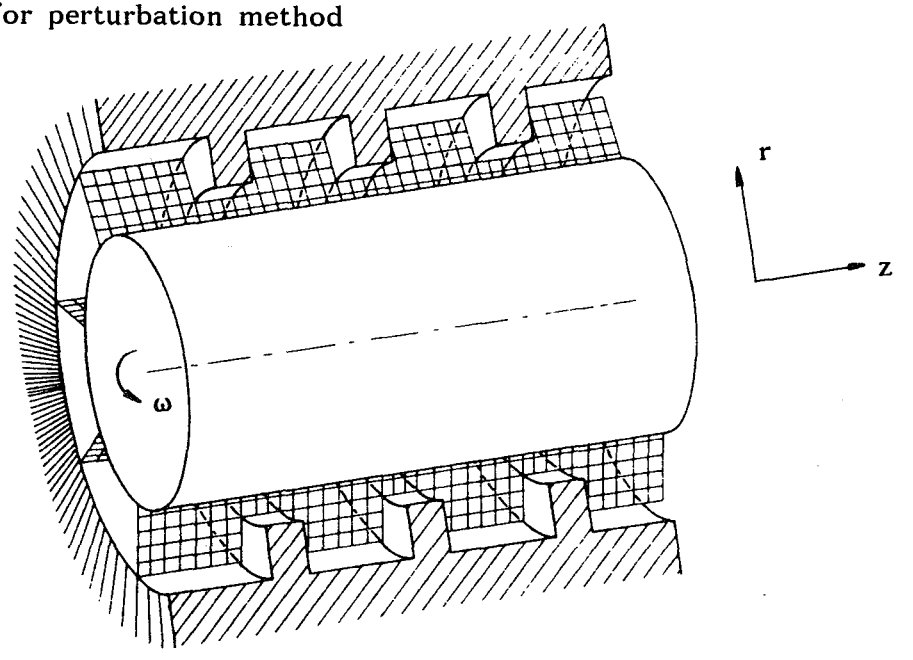

Fig. 4: 3D Finite Difference grid

In the next step, the generalized equation (2) is integrated over a control volume linking every node point with his neighbours in space. The resulting algebraic equations are then solved for the zeroth and first order equations (perturbation analysis) or the 3D equations respectively.

Finally, the dynamic forces are calculated from the pressure distribution on the rotor surface for two precession frequencies $\Omega=0$ and $\Omega=\omega$, resulting in two sets of forces. Then the dynamic coefficients are determined from eq. 1, where the prescribed circular shaft orbit is introduced:

$$- F_1 = r_o \, (K + \Omega d)$$
$$- F_2 = r_o \, (- k + \Omega D) \qquad (5)$$

For more detailed information concerning the perturbation analysis or the 3D algorithm, readers are referred to WEISER and NORDMANN /2,3/.

SIMPLIFIED METHODS

While the CFD algorithms require a lot of computer storage and cpu time, the simplified methods described in this chapter show a reduced effort to determine the rotordynamic labyrinth coefficients.

THREE VOLUME BULK FLOW MODEL

Following the conventional approach (see for example IWATSUBO /4/ or CHILDS /5/), a three volume bulk flow model has been developed based on the conservation equations for mass, momentum and energy working with velocities, pressure, density and temperature, which are averaged over the control volume height.
Flow visualization experiments show, that for look-through labyrinths, the flow field can be divided in two characteristic regions: a vortex flow in the seal chamber and a jet flow region beneath the seal strip and the groove. Therefore we use three control volumes (CV) to describe the flow situation in the labyrinth (Fig. 5).
To account for the flow turbulence, wall shear stresses and a fluid shear stress in the contact region of CV II and CV III are introduced. Following SCHARRER /6/, a vortex velocity in the chamber is assumed. The constants appearing in the shear stress formulations are determined with the aid of the CFD programs for centric shaft position.
Again, a perturbation analysis in connection with the implementation of solutions for the temporal and circumferential variation of the dependent variables is performed, resulting in the already known two sets of differential equations, which now depend only on the axial coordinate z. After their numerical solution, the forces and the dynamic seal coefficients are calculated by a pressure integration over the shaft surface.
More information concerning the bulk flow model can be found in NORDMANN and WEISER /7,8/.

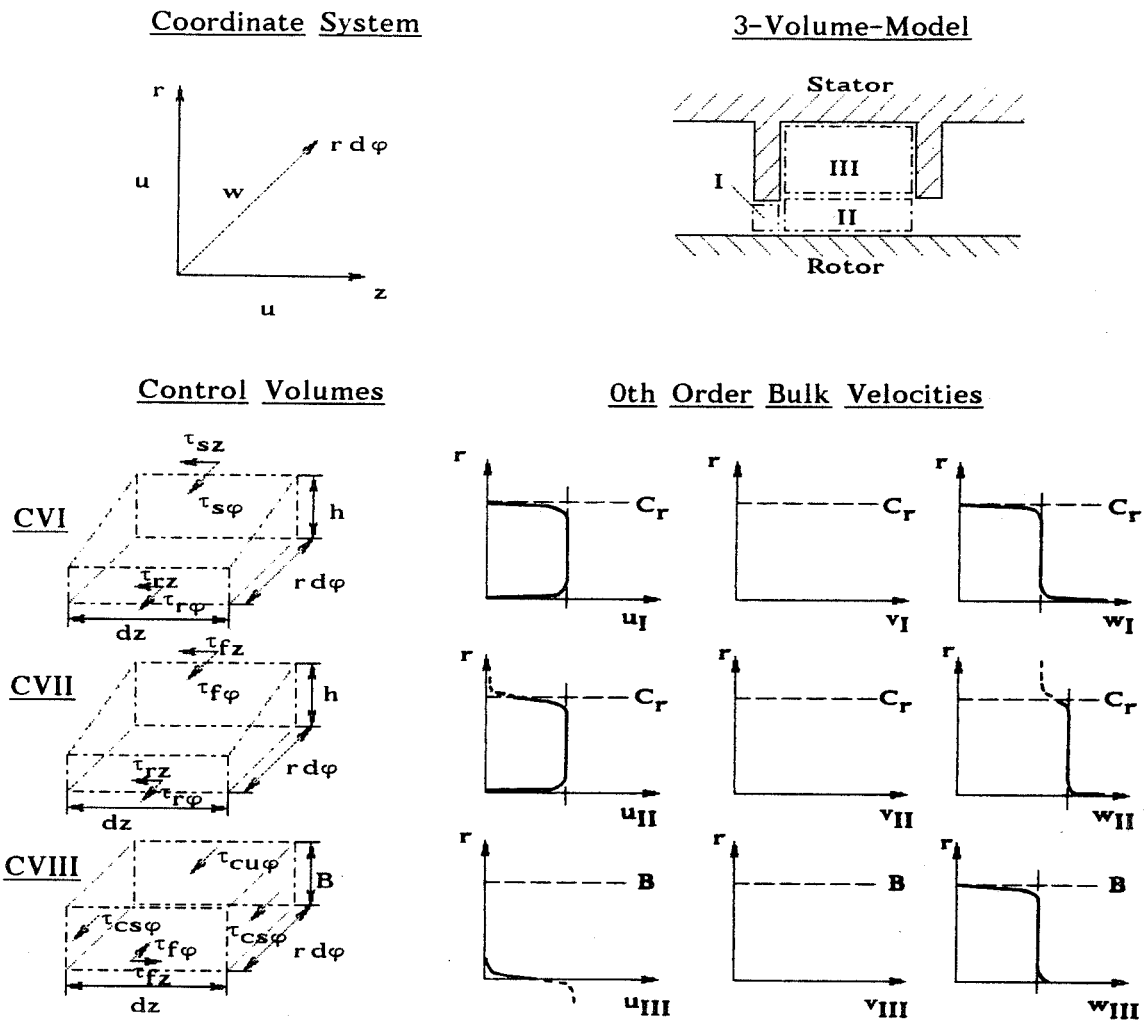

Fig. 5: Three volume bulk flow model

CORRELATION EQUATIONS FOR THE DYNAMIC COEFFICIENTS

Already in the design stage of a turbine or a compressor, the estimation of labyrinth coefficients is important for inclusion of these effects into rotordynamic calculations. Therefore, we developed approximation formulas for the desired stiffnesses and dampings to provide a tool for the design engineer, which can give some information about the rotordynamic seal influence to be expected. These correlations are based on extensive FD calculations for a model labyrinth, where performance data and geometry were varied in a wide range of practical interest.

First, the influence parameters which will be included in the correlation to perform must be defined (shown in Fig. 6).

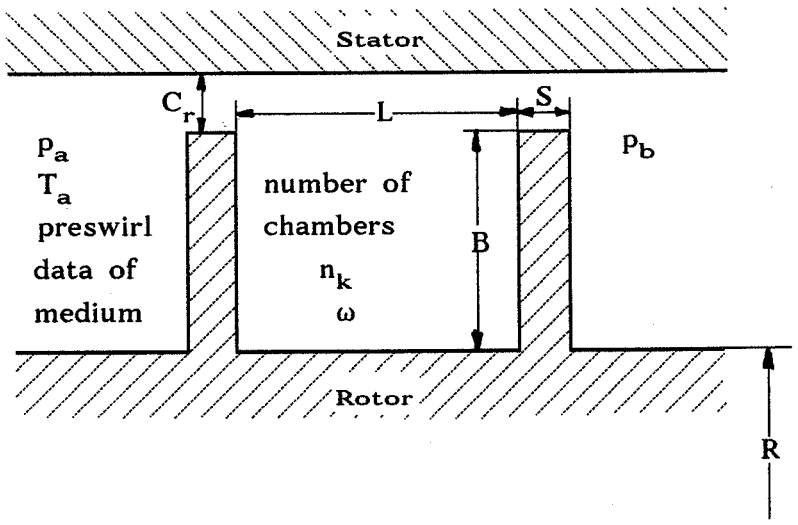

Fig. 6: Influence parameters for the correlation of dynamic coefficients

For the approximation equations, several definitions are used:

$$G = \alpha\, k_{ü}\, D_m\, C_r\, \pi\, G_{kr}\, q \qquad G_{kr} = \sqrt{9.80665\,\varkappa\left(\frac{2}{\varkappa+1}\right)^{\frac{\varkappa+1}{\varkappa-1}}}\ \sqrt{p_a\,\rho_a}$$

$$D_m = \frac{1}{2}\,\frac{2R + C_r + B\,m}{2} \qquad m = \begin{matrix} 0 : \text{Strips on stator} \\ 1 : \text{Strips on rotor} \end{matrix}$$

$$q = \begin{cases} n_k \geq 7: & \sqrt{\frac{1}{n_k}\,\frac{1-\varepsilon_z^2}{1-\varepsilon_{kr}} - \varepsilon_{kr}\,\frac{(1-\varepsilon_z^2)}{n_k^2\,(1-\varepsilon_{kr})^2}} \\ n_k \geq 7: & \sqrt{\frac{1}{n_k}\,\frac{1-\varepsilon_z^2}{1-\varepsilon_{kr}}} \end{cases} \qquad (6)$$

$$\alpha = \frac{\sqrt{14.44 - (C_r/S - 4)^2} - 26.656}{-33.32} \qquad \text{for } 0.2 \leq C_r/S < 4 \quad \text{and}$$

$$\alpha = 0.675 \qquad \text{for } C_r/S \geq 4$$

$$k_{ü} = \sqrt{\frac{n_k}{n_k(1-j_{ü})} + j_{ü}} \qquad j_{ü} = 1 - \left(1 + 16.6\,\frac{C_r}{L}\right)^{-2}$$

$$\varepsilon_z = \frac{p_b}{p_a} \qquad \varepsilon_{kr} = 0.528 \text{ (air)}$$

DESCRIPTION OF DIRECT STIFFNESS

The approximation for the direct stiffness consists of three parts:

- stiffness for axial flow situation (K_O)
- stiffness induced by shaft rotation (K_ω)
- stiffness induced by preswirl velocity (K_{w_i})

From FD calculations, we found that the influence of preswirl changes sign for labyrinths with more than 5 strips and that K becomes negative for multi-chamber seals. This is included in the following formulas:

$$K = K_O + K_\omega + K_{w_i} \qquad \text{for } n_k \leq 5$$

$$K = K_O + K_\omega - K_{w_i} \qquad \text{for } n_k > 5 \tag{7}$$

with

$$K_O = C_1^* \, f_g \, f_{n_k} \, f_p \, f_\tau$$

$$f_g = R \frac{L_S^2}{h_m^2}$$

$$f_p = (p_a - p_b)(1 + \zeta)$$

$$f_n = \begin{cases} (100 - 10 n_k) ; & n_k \geq 10 \\ (10 n_k - n_k^2) ; & n_k \leq 10 \end{cases}$$

$$f_\tau = \frac{\lambda}{\psi^2}$$

$$\lambda = \left(2(p_a - p_b) - \frac{G_S^2}{\rho_m A_s^2} \right) \frac{2 h_m \rho_m A_{sp}^2}{G_S^2 L_S}$$

$$\psi = \left(\frac{\lambda L_S}{2 h_m} + \zeta + 1 \right)$$

$$K_\omega = C_2^* \frac{p_a}{p_b} w_m$$

$$K_{w_i} = C_3^* \frac{p_a}{p_b} \left(\frac{w_i}{D_m} \right)^2$$

$A_{sp} = 2 \pi R C_r$

$h_m = 0.5 (B + C_r)$

$\rho_m = 0.5 (p_a + p_b) / (R_g T_a)$

$L_S = 4 L + 5 S$

G_S : Leakage for 5 strip Labyrinth

CROSS-COUPLED STIFFNESS

The cross-coupled stiffness is directly related to the leakage loss of the labyrinth. Also, the influence of geometry, shaft rotation and preswirl are included:

$$t_g = C_4^* \left(\frac{R}{C_r} \right)^2 \frac{L}{B}$$

$$t_{w,\omega} = \frac{2}{D_m} \left(w_i \left(n_k - \sqrt{2} \right) - w_m \left(n_k - 2.5 \right) D_m C_5^* \right) \qquad (8)$$

$$k = G\, t_g\, t_{w,\omega}$$

The average circumferential velocity w_m is determined using the 1/7-power law.

DIRECT DAMPING

To describe the direct damping D, some of the previously defined functions are used. The influence of shaft rotation, preswirl and geometry are found to be smaller than for the stiffnesses:

$$D = D_0 + D_\omega + |D_{w_i}|$$

$$D_0 = C_6^* f_g f_p f_\tau$$

$$D_\omega = C_7^* \frac{p_a}{p_b} w_m \qquad (9)$$

$$D_{w_i} = C_8^* \frac{p_a}{p_b} \frac{w_i}{D_m}$$

The correlation coefficients were determined from the FD calculation results for the data variations of the chosen model labyrinth:

$$C_1^* = 3.141\ 10^{-2} \quad C_2^* = 16.0\ \mathrm{Kg/(m\,s)} \quad C_3^* = 2.80\ 10^{-2}\ \mathrm{Kg}$$

$$C_4^* = \begin{cases} 4.2\ 10^{-3} & \text{(strips on rotor)} \\ 3.5\ 10^{-3} & \text{(strips on stator)} \end{cases} \quad C_5^* = 1.50\ \mathrm{m^{-1}} \quad C_6^* = 1.571\ 10^{-3}\ \mathrm{s}$$

$$C_7^* = 0.18\ \mathrm{N\,s^2/m^2} \quad C_8^* = 1.60\ 10^{-2}\ \mathrm{N\,s^2/m}$$

COMPARISON OF THE DIFFERENT APPROACHES WITH MEASUREMENTS

1. Example: A three chamber look-through labyrinth

To compare the two FDM, the bulk flow model and the correlation equations to measurements, we have chosen a look-through labyrinth which was experimentally investigated by BENCKERT /9/ (seal data given in /2/).

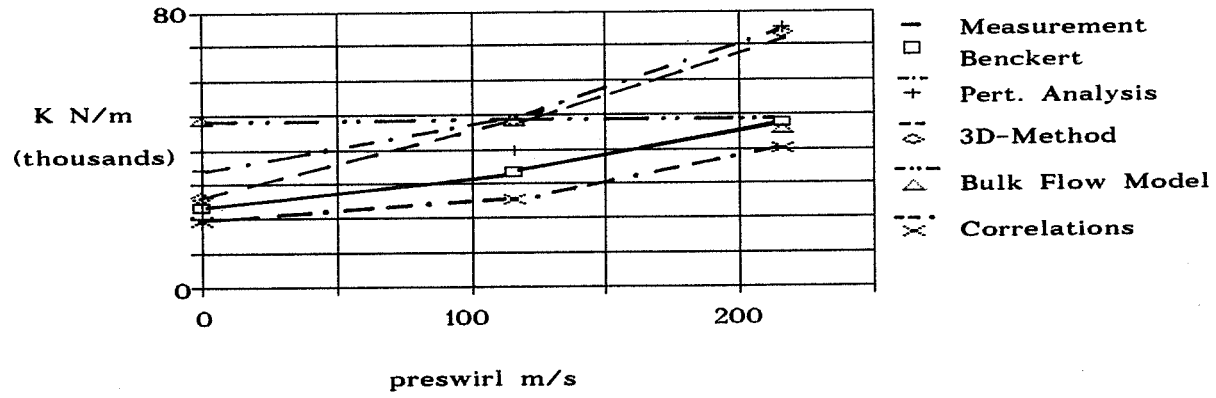

Fig. 7 : Direct Stiffness

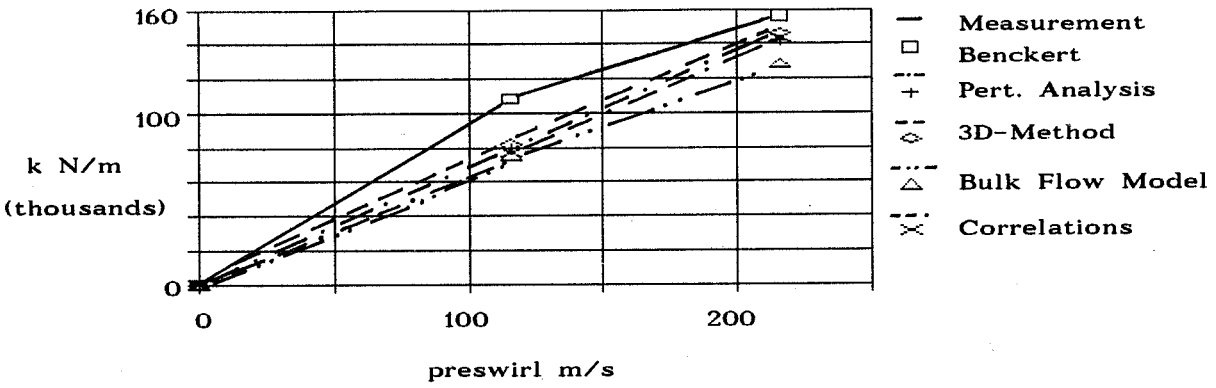

Fig. 8 : Cross-coupled Stiffness

2. Example: A multi-chamber look-through labyrinth seal

SCHMIED /10/ published experimental results obtained by CHILDS for a 12 strip stator labyrinth (seal data given in /10/). The comparisons in Fig. 9 - 11 show the results of perturbation analysis, bulk flow model and correlation for the stiffnesses and the direct damping.

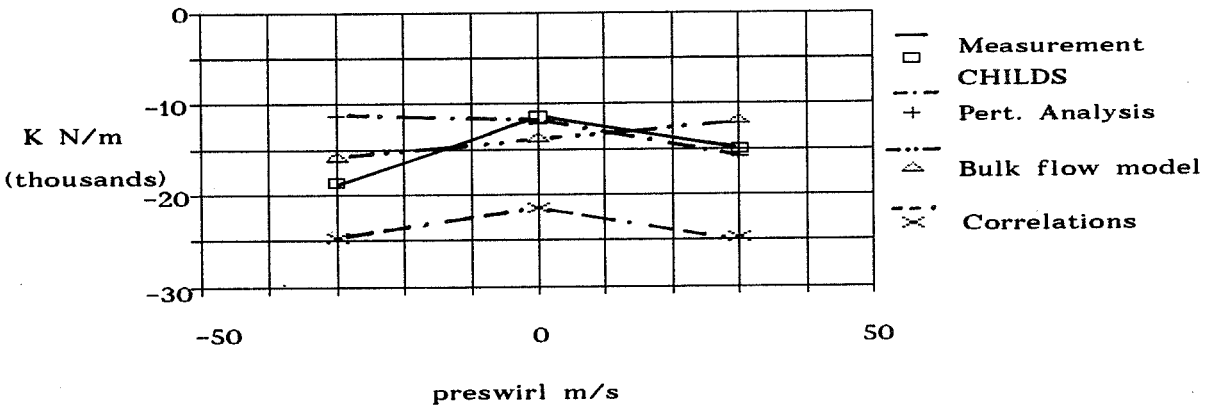

Fig. 9 : Direct Stiffness

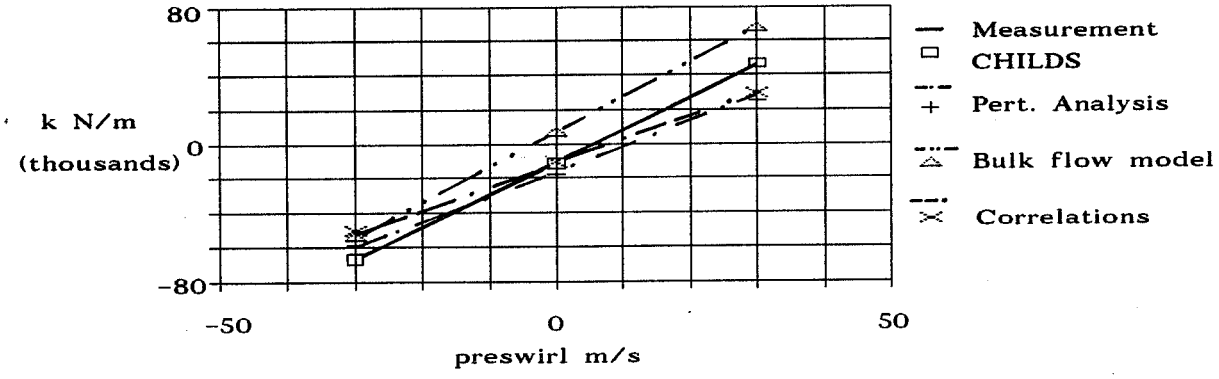

Fig. 10: Cross-coupled stiffness

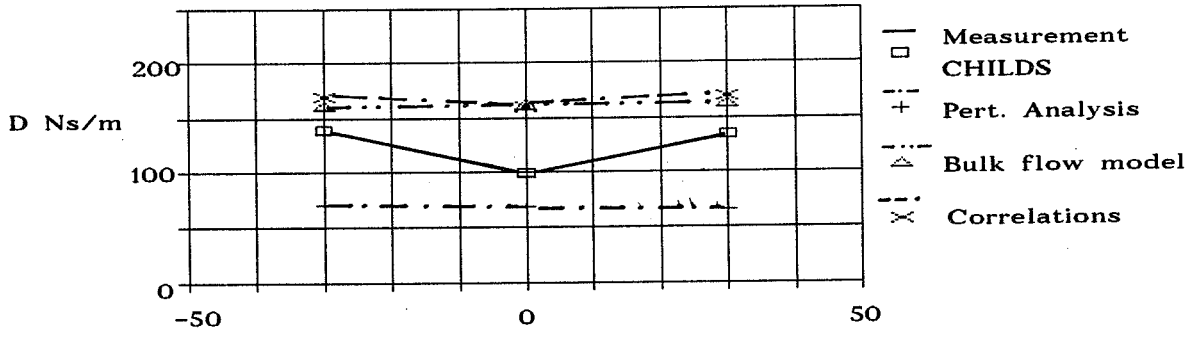

Fig. 11: Direct damping

APPLICATION OF SEAL DYNAMICS CALCULATION TO ROTORDYNAMIC DESIGN AND VIBRATION INVESTIGATIONS

In 1988, SCHMIED /10/ published rotordynamic calculations for a high performance injection compressor, where he included the most important fluid interaction influences coming from journal bearings, oil ring seals and labyrinths. Fig. 12 shows a sketch of the compressor rotor discretization and gives the basic data. The labyrinth data are given in /10/. SCHMIED uses the program MADYN to perform the eigenvalue calculations. In this chapter, a comparison is made to SCHMIEDs results for the first forward bending mode with straight through shroud and hub labyrinths, the comb-grooved balance piston and ideally floating oil ring seals.

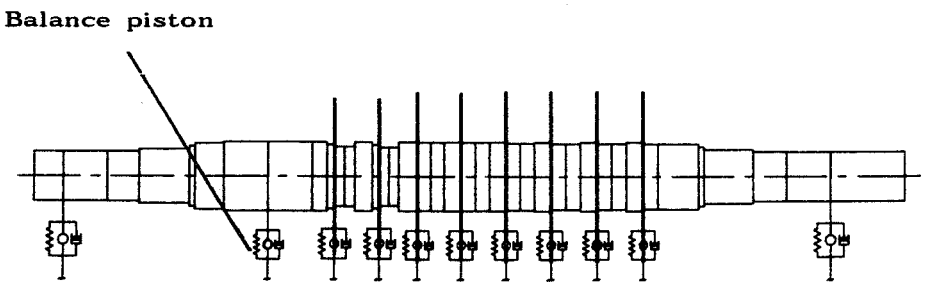

Basic compressor data:

Suction pressure:	198 bar	Mass flow:	47.5 kg/s	Op. speed:	13400 rpm
Discharge pressure:	700 bar	Rotor mass:	265 kg		
Mol. weight of gas:	20.05	Bearing dist.:	1565 mm		

Fig. 12: Investigated rotor

COMPARISON TO SCHMIED'S RESULTS FOR THE SIXTH STAGE SHROUD LABYRINTH

SCHMIED uses the labyrinth seal model of WYSSMANN /11/ to determine the rotordynamic coefficients. For the sixth stage shroud labyrinth, his calculations show negative direct stiffness values. As can be recognized in Fig. 13 to 15, the results of our investigations with the perturbation analysis, the bulk flow model and the correlation equations yield positive direct stiffness as expected. The agreement of cross-coupled stiffness and direct damping to the values obtained with WYSSMANNs theory is good. Especially, the different procedures presented in this paper are in relatively good agreement with each other for all rotordynamic parameters. This statement holds also true for all other labyrinth seals of the investigated compressor.

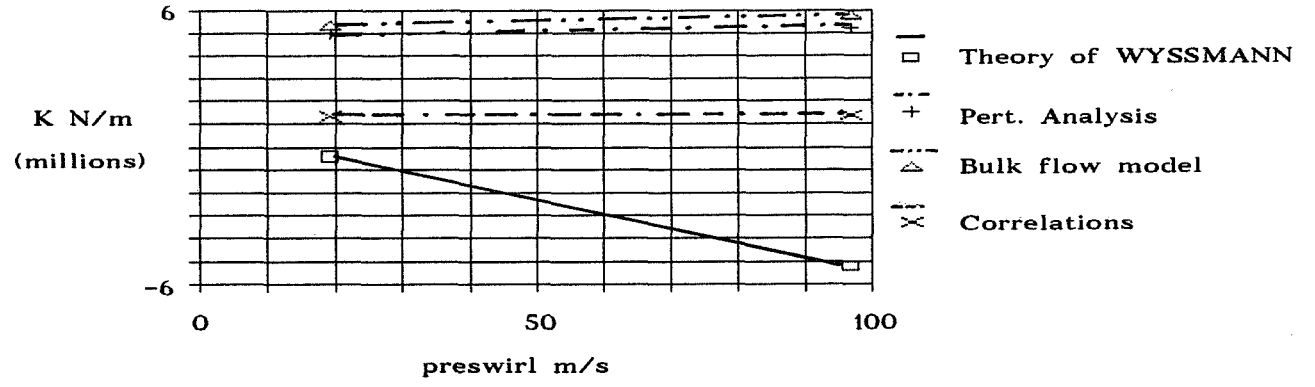

Fig. 13: Direct Stiffness

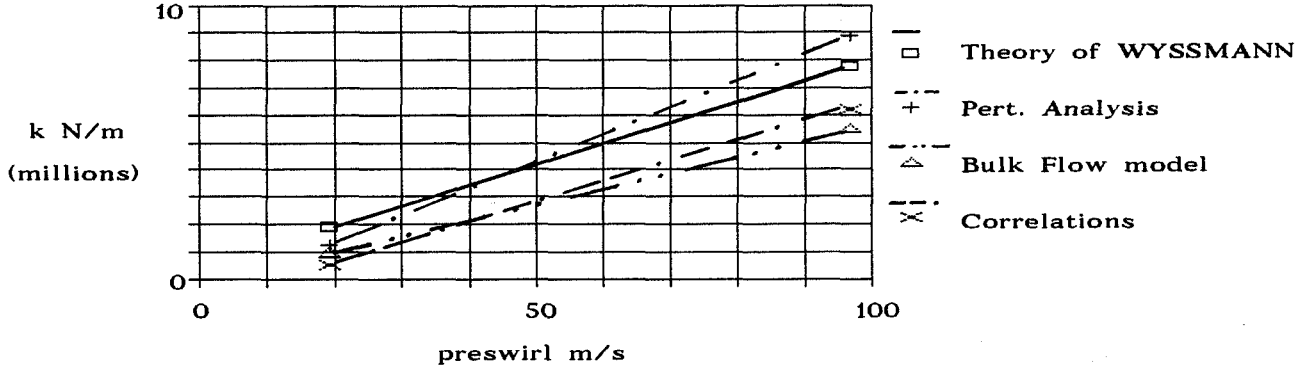

Fig. 14: Cross-coupled Stiffness

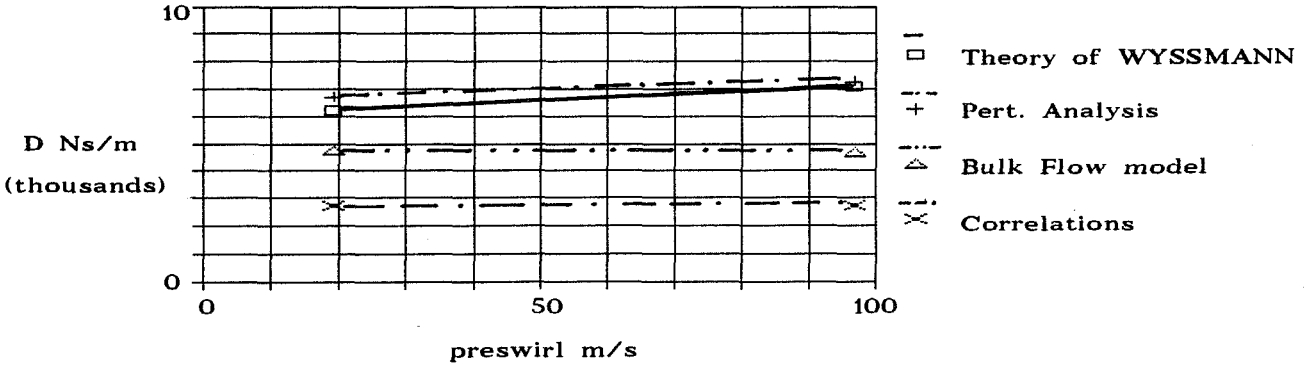

Fig. 15: Direct Damping

ROTORDYNAMIC ANALYSIS OF EIGENPROBLEM AND STABILITY

SCHMIED investigated three cases of rotordynamic interest:
- "ideal": rotor running in journal bearings, no labyrinth influence
- "with swirl brakes": labyrinth influence included for low preswirl conditions
- "without swirl brakes": labyrinth influence included for high preswirl conditions

For these cases, we have calculated the eigenfrequencies and modal dampings of the rotor system using the Finite-Element program of DIEWALD /12/ . In Fig. 16 and 17, comparisons are presented for the first forward bending mode. For the "ideal" system, the calculations show nearly the same results. Because of the labyrinth coefficients obtained with the FD perturbation analysis for the hub and shroud labyrinths and the bulk flow model for the balance piston, the first eigenfrequency is higher than in SCHMIEDs calculations. This is mainly due to the positive direct stiffnesses for the impeller labyrinths. Also the modal damping shows great differences.

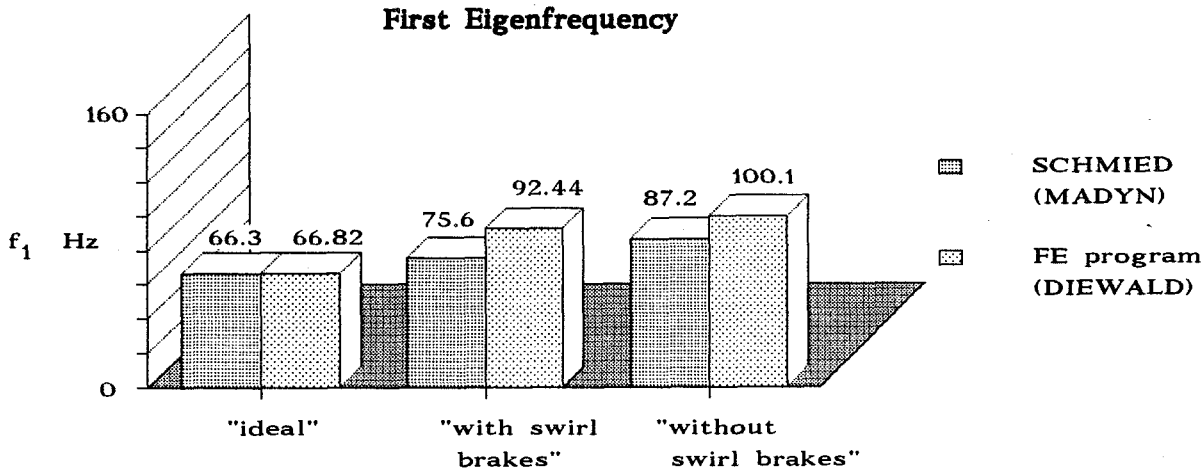

Fig. 16: Comparison of first eigenfrequency

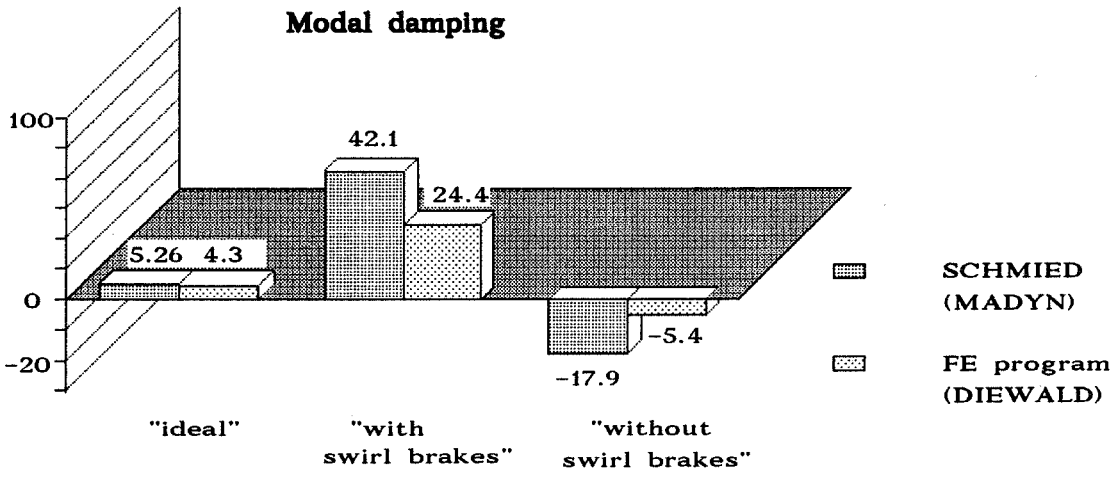

Fig. 17: Modal damping of first forward bending mode

CONCLUSION

Four calculation methods have been described allowing calculation of the dynamic labyrinth coefficients. Comparisons to experiments show good agreement for all methods and all investigated cases.

The practical example of rotordynamic calculations for a high-performance compressor has shown that the determination of labyrinth coefficients must be performed as exactly as possible in order to predict the eigenfrequencies and modal dampings correctly. Also, it has been proved that the methods presented in this paper are superior for this task to the existing theories.

LITERATURE

/1/ LAUNDER, B. E., SPALDING, D. B.:
"The Numerical Computation of Turbulent Flows"
Computer Methods in Applied Mechanics and Engineering 3,
(1974), S. 269 - 289

/2/ NORDMANN, R., WEISER, H.P.:
"Rotordynamic Coefficients for Labyrinth Seals Calculated by Means of a Finite-Difference Technique"
NASA CP 3026, 1988

/3/ WEISER, H. P., NORDMANN, R.:
"Calculation of Rotordynamic Labyrinth Seal Coefficients by Means of a Threedimensional Finite-Difference Method"
Biennial Conference on Mechanical Vibration and Noise, Montreal 1989

/4/ IWATSUBO, T.; TAKAHARA, K.; KAWAI, R.:
"A New Model of Labyrinth Seal for Prediction of the Dynamic Force"
NASA CP 2338, 1984

/5/ CHILDS, D. W., SCHARRER, J. K.:
"An Iwatsubo-Based Solution for Labyrinth Seals - Comparison with Experimental Results"
NASA CP 2338, 1984

/6/ SCHARRER, J. K.:
"Theory versus Experiment for the Rotordynamic Coefficients of Labyrinth Gas Seals: Part I - A Two Control Volume Model"
The 11th Biennial Conference on Mechanical Vibrations and Noise, Boston, 27-30 Sept. 1987

/7/ NORDMANN, R.; WEISER, H.P.:
"A Three Volume Bulk Flow Model for the Calculation of Rotordynamic Coefficients of Look-Through Labyrinths"
Third International Symposium on Transport Phenomena and Design of Rotating Machinery, Honolulu, USA, 1990

/8/ NORDMANN, R.; WEISER, H.P.:
"Evaluation of Rotordynamic Coefficients of Look-Through Labyrinths by Means of a Three Volume Bulk Flow Model"
The Sixth Workshop on Rotordynamic Instability Problems in High Performance Turbomachinery, College Station Texas, USA, 1990

/9/ BENCKERT, H.:
"Strömungsbedingte Federkennwerte in Labyrinthdichtungen"
Dissertation TU Stuttgart, 1980

/10/ SCHMIED, J.:
"Rotordynamic Stability Problems and Solutions in High Pressure Turbocompressors"
NASA CP 3026, 1988

/11/ WYSSMANN, H. R., PHAM, T. C., JENNY, R. J.:
"Prediction of Stiffness and Damping Coefficients for Centrifugal Compressor Labyrinth Seals"
ASME Journal of Engineering for Gas Turbines and Power, Okt. 1984, B. 106, S. 920 - 926

/12 DIEWALD, W., NORDMANN, R.:
"Dynamic Analysis of Centrifugal Pump Rotors with Fluid-Mechanical Interactions"
11th Biennial Conference on Mechanical Vibration and Noise, Boston, 27-30 Sept. 1987